BIOMOLECULES & THERAPEUTICS

Original Article
Biomol Ther 32(1), 65-76 (2024)

Bortezomib Is Toxic but Induces Neurogenesis and Inhibits TUBB3 Degradation in Rat Neural Stem Cells

Seung Yeon Sohn, Thin Thin San, Junhyung Kim and Hyun-Jung Kim*

College of Pharmacy, Chung-Ang University, Seoul 06974, Republic of Korea

Abstract

Bortezomib (BTZ) is a proteasome inhibitor used to treat multiple myeloma (MM). However, the induction of peripheral neuropathy is one of the major concerns in using BTZ to treat MM. In the current study, we have explored the effects of BTZ (0.01-5 nM) on rat neural stem cells (NSCs). BTZ (5 nM) induced cell death; however, the percentage of neurons was increased in the presence of mitogens. BTZ reduced the B-cell lymphoma 2 (Bcl-2)/Bcl-2 associated X protein ratio in proliferating NSCs and differentiated cells. Inhibition of βIII-tubulin (TUBB3) degradation was observed, but not inhibition of glial fibrillary acidic protein degradation, and a potential PEST sequence was solely found in TUBB3. In the presence of growth factors, BTZ increased cAMP response element-binding protein (CREB) phosphorylation, brain-derived neurotrophic factor (*Bdnf*) transcription, BDNF expression, and *Tubb3* transcription in NSCs. However, in the neuroblastoma cell line, SH-SY5Y, BTZ (1-20 nM) only increased cell death without increasing CREB phosphorylation, *Bdnf* transcription, or TUBB3 induction. These results suggest that although BTZ induces cell death, it activates neurogenic signals and induces neurogenesis in NSCs.

Key Words: Ubiquitin-proteasome system, Bortezomib, Rat neural stem cells, Neurodegenerative disease, Apoptosis, Protein degradation

INTRODUCTION

Proteins mediate cellular function; therefore, the generation, maintenance, and degradation of proteins result in distinct repertoire in cells to control biological effects (Martinez-Vicente *et al*., 2005; Ye, 2018). In cells, protein degradation is precisely regulated by lysosomes and proteasomes (Ciechanover, 2005; Cohen-Kaplan *et al*., 2016; Nam *et al*., 2017). The 26S Proteasome recognizes ubiquitylated proteins for degradation, however, the substrate size matters since ubiquitylated proteins have to enter the catalytic 20S core unit, which has a 19S regulatory cap at one or both ends (Bach and Hegde, 2016; Pohl and Dikic, 2019). Substrate proteins prone to degradation are tagged by ubiquitin, and this process is modulated by several steps of enzymatic reactions (Pohl and Dikic, 2019).

Dysfunction or dysregulation of protein degradation systems, including proteasomes is involved in pathological conditions such as cancers and neurodegenerative diseases (Paul, 2008; Vilchez *et al*., 2014; Kaushik and Cuervo, 2015). Proteasome inhibitors (PIs), including bortezomib (BTZ; Velcade), are used to treat multiple myeloma (MM), mantle cell lymphoma, and autoimmune diseases (Robak and Robak, 2019; Thibaudeau and Smith, 2019). However, peripheral neuropathy (PN) is prevalently observed in patients treated with PIs (Velasco *et al*., 2019). BTZ is the first approved drug that inhibits proteasome to treat MM, and about 50% of patients who received BTZ developed PN (Adams, 2003; Richardson *et al*., 2009; Chen and Dou, 2010; Dick and Fleming, 2010; Velasco *et al*., 2010; Robak and Robak, 2019). Increased stability of microtubules by PIs might be responsible for the increased incidence of PN (Poruchynsky *et al*., 2008; Pero *et al*., 2021), however, the mechanisms related to PN induction via PIs are not clearly known yet.

Neural stem cells (NSCs) are found in the developing and adult nervous systems and are an efficient tool for studying neural development, drug development, and toxicity (Kong *et al*., 2018; Lee *et al*., 2019; Kim and Kim, 2020; Lee *et al*., 2021). NSCs can proliferate in response to growth signals and differentiate into neurons or glia in the presence of differentiation stimulus or removal of growth factors in the media (Kim *et al*., 2007; Lee *et al*., 2016). In the current study, we

Open Access **https://doi.org/10.4062/biomolther.2023.134**

Received Jul 24, 2023 **Revised** Oct 17, 2023 **Accepted** Oct 25, 2023
Published Online Dec 11, 2023

***Corresponding Author**
E-mail: hyunjungkim@cau.ac.kr
Tel: +82-2-820-5619, Fax: +82-2-816-7338

explored the effect of BTZ on NSC survival and fate control. We have found that BTZ induced cell death, inhibited degradation of βIII-tubulin (TUBB3), and interestingly, increased neurogenesis (neuronal differentiation) in the presence of mitogens. These effects were specific to NSCs because in differentiated cells and neuroblastoma SH-SY5Y cells, the activation of cAMP response element-binding protein (CREB) phosphorylation and transcriptional activation of brain-derived neurotrophic factor (BDNF) were not observed. In addition, the degradation of TUBB3 by the proteasome appeared to be mediated by a specific PEST amino acid sequence.

MATERIALS AND METHODS

Chemicals

The PI BTZ (504314) and dimethyl sulfoxide (DMSO) (472301) were purchased from Sigma-Aldrich (Saint Louis, MO, USA). BTZ was diluted to a stock solution of 50 μM using DMSO and stored at –20°C.

Cell culture and media

NSCs were extracted from the cortex of embryonic day 14 (E14) Sprague-Dawley rat embryos (Orient Bio, Seongnam, Korea). After a brief exposure to CO_2, the animals were anesthetized and sacrificed by cervical dislocation as previously described (Lee *et al*., 2019). Animal experiments were conducted with permission from the Animal Care of Chung-Ang University (authorization code: 13-0049, 2014-00032) along with the NIH Guidelines for the Care and Use of Laboratory Animals. NSCs were cultured (200,000 cells/mL) in 25 cm^2 flasks (BD Falcon-Corning, Corning, NY, USA). NSCs were grown for 7 days to expand into neurospheres in dulbecco's modified eagle medium/F12 (DMEM/F12) supplemented with 1% (v/v) antibiotic-antimycotic, 2% (v/v) B27 (12500-062; 15240-062; 17504-044; all from Gibco-Thermo Fisher Scientific, Waltham, MA, USA), 20 ng/mL epidermal growth factor (EGF) and 20 ng/mL fibroblast growth factor 2 (FGF2) (GF144; GF003AF; both from Merck Millipore, Burlington, MA, USA). NSCs were cultured in an incubator at 37°C in 5% CO_2, and the medium was replaced every 2 days. Neurospheres were then dissociated with accutase (SCR005; Chemicon, Merck KGaA, Darmstadt, Germany) into a single cell suspension and seeded on plates for 1 day culture. Before seeding cells, plates were coated with 0.01% poly-D-lysine (P0899; Sigma-Aldrich) overnight and 10 μg/mL laminin (23017-015; Invitrogen, Carlsbad, CA, USA). NSCs were cultured without EGF and FGF2 to induce differentiation and treated with 0.1% DMSO, BTZ (0.01-5 nM) or 10 ng/mL recombinant rat ciliary neurotrophic factor (CNTF) (GF035; Chemicon, Merck KGaA).

The human neuroblastoma SH-SY5Y cell line (KCLB number: 22266, passage number: k27) was provided by the Korean Cell Line Bank (Seoul, Korea). After thawing SH-SY5Y cells, they were maintained in DMEM/F12 supplemented with 10% (v/v) heat-inactivated fetal bovine serum (S001-07; Welgene, Gyeongsan, Kore) and 1% (v/v) antibiotic-antimycotic at 37°C in 5% CO2. The growth medium was changed every 3 days. When the cells reached 70% confluency, they were treated with BTZ (1-20 nM) or 0.1% DMSO as a control. For passaging, the cells were detached using 500 μL of 0.25% trypsin-EDTA (25200-056; Gibco-Thermo Fisher Scientific) for 5 min. An equal amount of growth medium was added to neutralize the trypsin. Cells were subcultured until passage 8, frozen in a cryotube with 5% DMSO in growth media and stored in liquid nitrogen.

Western blot analysis

NSCs and SH-SY5Y cells were rinsed with phosphate-buffered saline (PBS) before collection. Cells were lysed with a lysis buffer (50 mM NaCl, 5 mM EDTA, 50 mM HEPES) [all from VWR (Amresco), Solon, OH, USA] containing Halt Phosphatase Inhibitor Cocktail (78420; Thermo Fisher Scientific, Waltham, MA, USA), 1 mM phenylmethylsulfonyl fluoride, 0.01 mg/mL leupeptin, and 0.01 mg/mL aprotinin (P7626; A1153; L9783; all from Sigma-Aldrich). The protein concentration was measured using a Pierce™ BCA protein assay kit (23227; Thermo Fisher Scientific), and lysates were heated for 5 min. Protein lysates were mixed with a sodium dodecyl sulfate (SDS) sample buffer (60 mM Tris-HCl of pH 6.8, 25% glycerol, 2% SDS, 0.1% bromophenol blue) [all from VWR (Amresco)], 14.4 mM β-mercaptoethanol (M6250; Bio-Rad, Hercules, CA, USA), and distilled water. The proteins were separated on a 10%-15% SDS-polyacrylamide electrophoretic gel and transferred to polyvinylidene fluoride membranes (ISEQ00010; Millipore, Merck KGaA) for 1 h. Precision Plus Protein™ Ladder (#161-0374; Bio-Rad) was used to estimate the size of each protein. The membranes were blocked with 5% skim milk or bovine serum albumin (82100-6; Merck Millipore) in tris-buffered saline (TBS) with 0.03% or 0.1% tween 20 [M147; VWR (Amresco)] (TBST) for 1 h and incubated overnight at 4°C with primary antibodies: anti-TUBB3 known as TuJ1 (1:1000; T5076), anti-glial fibrillary acidic protein (GFAP) (1:500; G9269; both from Sigma-Aldrich), anti-B-cell lymphoma 2 (Bcl-2) (1:100; sc-7382; Santa Cruz, Dallas, TX, USA), anti-bcl-2 associated X protein (Bax) (1:1000; #2772; Cell Signaling, Danvers, MA, USA), anti-ubiquitin (P4D1) (1:1000; #3936; Cell Signaling), anti-BDNF (1:1000; ab108319; Abcam, Cambridge, MA, USA), anti-phospho-CREB (p-CREB) (Ser133) (1:1000; #06-519; Merck Millipore), anti-total-CREB (1:1000; #9197; Cell Signaling) and for internal control detected by anti-glyceraldehyde 3-phosphate dehydrogenase (GAPDH) (1:1000; sc-32233; Santa Cruz). After incubating overnight, membranes were washed 3 times with 0.03% TBST and incubated in horseradish peroxidase-conjugated secondary antibodies: anti-mouse IgG (1:5000; ADI-SAB-100-J), or anti-rabbit IgG (1:5000; ADI-SAB-300-J; both from Santa Cruz) for 1 h. Immunopositive protein bands were visualized on an X-ray film (CP-BU NEW; Agfa, Mortsel, Belgium) by enzyme activation using Western Blotting Luminol Reagent (Santa Cruz).

Real-time quantitative reverse transcription-polymerase chain reaction (Real-time qRT-PCR)

Total RNA (1 μg) was extracted using TRIzol reagent (15596026; Invitrogen) and was used for reverse-transcription of first strand cDNA with QuantiTect Reverse Transcription Kit (205313; Qiagen, Venlo, Limburg, Netherlands). Real-time PCR was performed after RT-PCR to quantify mRNA using iQ SYBR Green Supermix (#1708882AP; Bio-Rad). Specific primer sets were obtained from (Cosmo Genetech, Seoul, Korea) and used to amplify the cDNA as follows: *Tubb3* (Rat), agccctctacgacatctgct (forward), attgagctgaccagggaatc (reverse); *Gfap* (Rat), agcggctctgagagagattc (forward), agcaacgtctgtgaggtctg (reverse); *Bcl-2* (Rat), tgacttctctcgtcgctacc

(forward), gaactcaaagaaggccacaa (reverse); *Bax* (Rat), tggttgccctttctactttg (forward), gaagtaggaaaggaggccatc (reverse); *Bdnf* (Rat), gcccaacgaagaaaaccataag (forward), gtttgcggcatccaggtaatt (reverse); *Bdnf* (Human), taacggcggcagacaaaaaga (forward), gaagtattgcttcagttggcct (reverse); *Gapdh* (Rat), agttcaacggcacagtcaag (forward), gtggtgaagacgccagtaga (reverse); *Gapdh* (Human), ggtctcctctgacttcaaca (forward), agccaaattcgttgtcatac (reverse). The housekeeping gene *Gapdh* was used as an internal control. The conditions of each step for the PCR reaction were as follows: initial activation was started at 95°C for 3 min, then 40 cycles of denaturation at 95°C for 10 s, followed by annealing at 58°C for 15 s, and extension at 72°C for 20 s. Reaction data were analyzed using Bio-Rad CFX Manager 3.1.

Immunocytochemistry (ICC)

NSCs were fixed with 4% paraformaldehyde (P2031; Biosesang, Seongnam, Korea) for 30 min. Fixed cells on coverslips were blocked with PBS containing 5% normal goat serum (S26, Merck Millipore) and 0.2% triton X-100 [VWR (Amresco)] for 30 min and then incubated with primary antibodies: TuJ1 (1:1000; mouse IgG2b; T5076, Sigma-Aldrich), or anti-GFAP (1:500; rabbit IgG; Z0334, Agilent, Santa Clara, CA, USA) for 1 h 30 min. After washing with PBS, secondary antibodies conjugated to Alexa Fluor 488 (1:1000; goat anti-mouse IgG; A11001; Thermo Fisher Scientific), or Cy3 (1:1000; goat anti-rabbit; 111-165-144; Jackson ImmunoResearch, West Grove, PA, USA) were incubated for 30 min and then the cells were rinsed with PBS. 4',6-diamidino-2-phenylindole (DAPI) (1:1000; D9542, Sigma-Aldrich) was used for staining the nuclei. Images of each sample were acquired with an inverse fluorescence microscope (DMIL; Leica, Wetzlar, Germany) and were taken from three random fields for each condition. The percentage of positive staining was calculated by the number of TuJ1-, or GFAP- positive cells divided by the total DAPI-positive cells of each condition.

Time-lapse microscopy

NSCs were plated and cultured in the presence of mitogen. After 24 h, NSCs were cultured in media with 5 nM BTZ and mitogens. Time-lapse images were obtained every 20 min for 24 h with Incucyte S3 live-cell imaging system (Sartorius, Göttingen, Germany). Fluorescence image was obtained with Incucyte S3 live-cell imaging system (Sartorius). Cell tracking was performed manually in Fiji using TrackMate plugin (https://doi.org/10.1016/j.ymeth.2016.09.016).

Neurosphere growth rate

Measurement of neurosphere growth has been previously described (Kim *et al*., 2009; Kong *et al*., 2015; Kim and Kim, 2020). Each sphere (around 100-200 μm in diameter) was relocated to a single well into 96-well plates. Individual wells contained 200 μL of growth media supplemented with growth factors. The diameter of the spheres treated with BTZ or DMSO was estimated daily (day 0-4) by a ruler on a lens-mounted microscope (Leica). To calculate sphere volume in response to treatment, the volume of each neurosphere was divided by that of the sphere on day 0 and then multiplied by 100. In detail, the volume was estimated by the equation $V=4/3\pi r^3$, $r=1/2$ diameter, as previously described (Kim and Kim, 2020).

Cell viability assay

A 3-(4,5-dimethylthiazol-2-yl)-2,5-diphenyltetrazolium bromide (MTT) (M5655; Sigma-Aldrich) assay was conducted to measure the cell viability of SH-SY5Y cells. Cells were seeded in 48-well plates with growth media. When the cells reached 70% confluency, they were treated with DMSO or BTZ. After 2 days of treatment, MTT solution (1 mg/mL) was added to the media and left to incubate for 2 h at 37°C to form formazan crystals. Lysis buffer composed of 20% SDS [0227; VWR (Amresco)] in 50% aqueous N, N-dimethylformamide (D4551; Sigma-Aldrich) was added to solubilize formazan for 30 min. Lysates were transferred to 96-well plates, and absorbance was estimated at 550 nm by a Synergy H1 Hybrid Multi-Mode microplate reader (Biotek, Winooski, VT, USA).

Statistical analysis

All experiments were carried out with three independent biological replicates. Data were indicated as mean ± standard error of the mean (SEM). The graphs were generated using Sigma plot 10.0 (Systat Software, Inc., Palo Alto, CA, USA). Statistical significance was determined by Student's *t*-test (*$p<0.05$, **$p<0.01$).

RESULTS

BTZ is toxic but increases neurogenesis in proliferating NSCs

NSCs obtained from the cortex of E14 rats proliferate in the presence of growth factors and differentiate into neurons and glia in the absence of growth factors (Kong *et al*., 2015, 2018). To explore how the PI BTZ affects NSC fate or survival during proliferation, we treated NSCs with BTZ (0.01, 0.1, 1, and 5 nM) for 24 h in the presence of EGF and FGF2 (Fig. 1A-1H). We performed ICC using antibodies that detect neuronal marker protein TUBB3 (TuJ1 antibody) and anti-GFAP that identifies astrocytes. Nuclei were stained with DAPI to obtain the total number of cells. As shown in Fig. 1A and 1B, representative photographs show that, in the BTZ (5 nM)-treated condition, the number of DAPI-stained nuclei was significantly reduced compared with that of the DMSO control. These suggest that BTZ inhibits NSC proliferation or is inducing cell death (Fig. 1A-1C). Interestingly, BTZ significantly increased the percentage of neurons in a concentration-dependent manner (Fig. 1D). BTZ treatment did not enhance the percentage of astrocytes (Fig. 1E). In addition, the expressions of both *Tubb3* mRNA and TUBB3 protein were increased in 5 nM BTZ-treated NSCs (Fig. 1F, 1H). BTZ did not alter the expression of *Gfap* mRNA nor the protein expression (Fig. 1G, 1I). These data suggest that BTZ increases neurogenesis in proliferating NSCs although it induces cell death or inhibits NSC proliferation.

Next, we treated NSCs with BTZ for 4 days in the absence of mitogens and performed ICC to investigate the effect of BTZ during NSC differentiation. Similar to the data obtained from proliferation condition, treatment with 5 nM BTZ during differentiation significantly reduced the number of nuclei, and the percentage of neurons and astrocytes, suggesting that 5 nM BTZ decreases cell number in differentiated cells (Fig. 2A-2E). However, 1 nM BTZ did not induce cell count decrease determined by the morphology and the number of nuclei, in addition, different from the proliferating condition, 1 nM BTZ

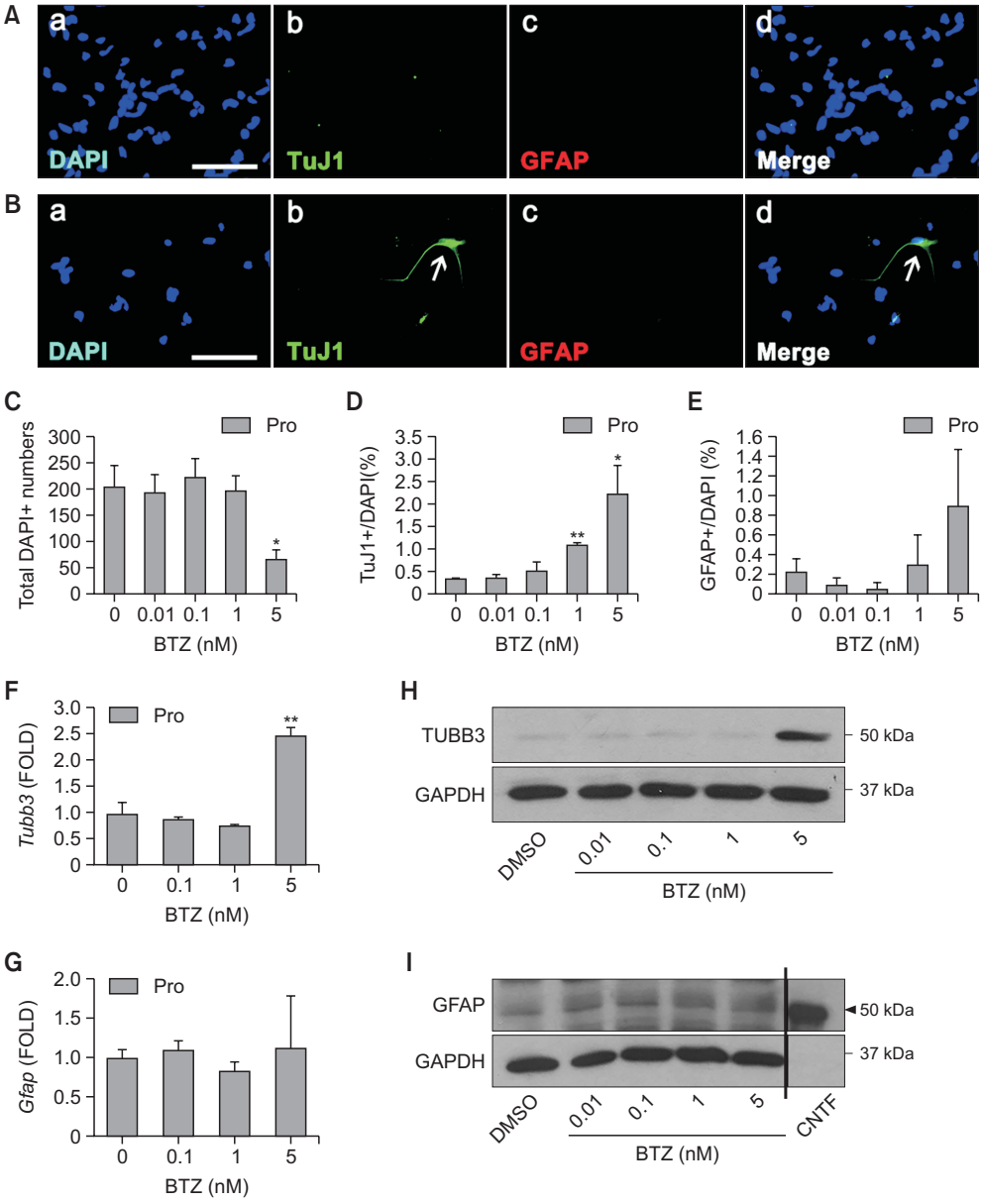

Fig. 1. BTZ increases the percentage of neurons in the presence of growth factors in NSCs. (A-E) NSCs were treated with 0.1% DMSO or 0.01, 0.1, 1, and 5 nM BTZ in the presence of EGF and FGF2 for 24 h. (A, B) Immunofluorescence images of NSCs treated with (A) DMSO or (B) 5 nM BTZ showing (a) nuclei stained with DAPI (blue), (b) neurons stained with TuJ1, (c) astrocytes stained with GFAP (red), and (d) the merged images. Neurons are indicated by the arrows (→). Scale bar=50 μm. (C-E) Quantification of (C) nuclei, (D) TuJ1- and (E) GFAP-positive cells. (F, G) RT-PCR was performed to quantify mRNA levels of *Tubb3* and *Gfap*. Total RNA was extracted from NSCs treated with 0.1% DMSO or 0.1, 1, and 5 nM BTZ for 24 h in the presence of EGF and FGF2. *Gapdh* was used as an internal control. (H, I) Representative images of protein bands of (H) TUBB3 and (I) GFAP. After 24 h of treatment in the presence of EGF and FGF2, total cell lysates were collected, and a western blot analysis was conducted with TuJ1 and GFAP antibodies. GAPDH was used as a loading control. CNTF was used as a positive control for GFAP. Data are presented as the mean ± SEM (n=3). **p*<0.05, ***p*<0.01 (Student's *t*-test). Uncropped images of western blots are shown in Supplementary Fig. 1.

did not increase the percentage of neurons (Fig. 2C, 2D). During differentiation, low concentrations of BTZ (0.01-1 nM) did not affect astrocytogenesis (Fig. 2E). Real-time PCR results showed that BTZ had differential effects on NSCs depending on the presence of EGF and FGF2. In the presence of these mitogens, BTZ (5 nM) increased *Tubb3* transcripts (Fig. 1F). However, when NSCs were treated with BTZ in the absence of EGF and FGF2 to facilitate differentiation, the mRNA level of *Tubb3* was not altered (Fig. 2F). These results indicate that BTZ up-regulates Tubb3 mRNA in proliferating NSCs but not in differentiating cells. The expression level of *Gfap* transcripts was not affected by BTZ (Fig. 2G). The protein expression level of TUBB3 was increased but that of GFAP was not altered by BTZ in the absence of EGF and FGF2 (Fig. 2H, 2I).

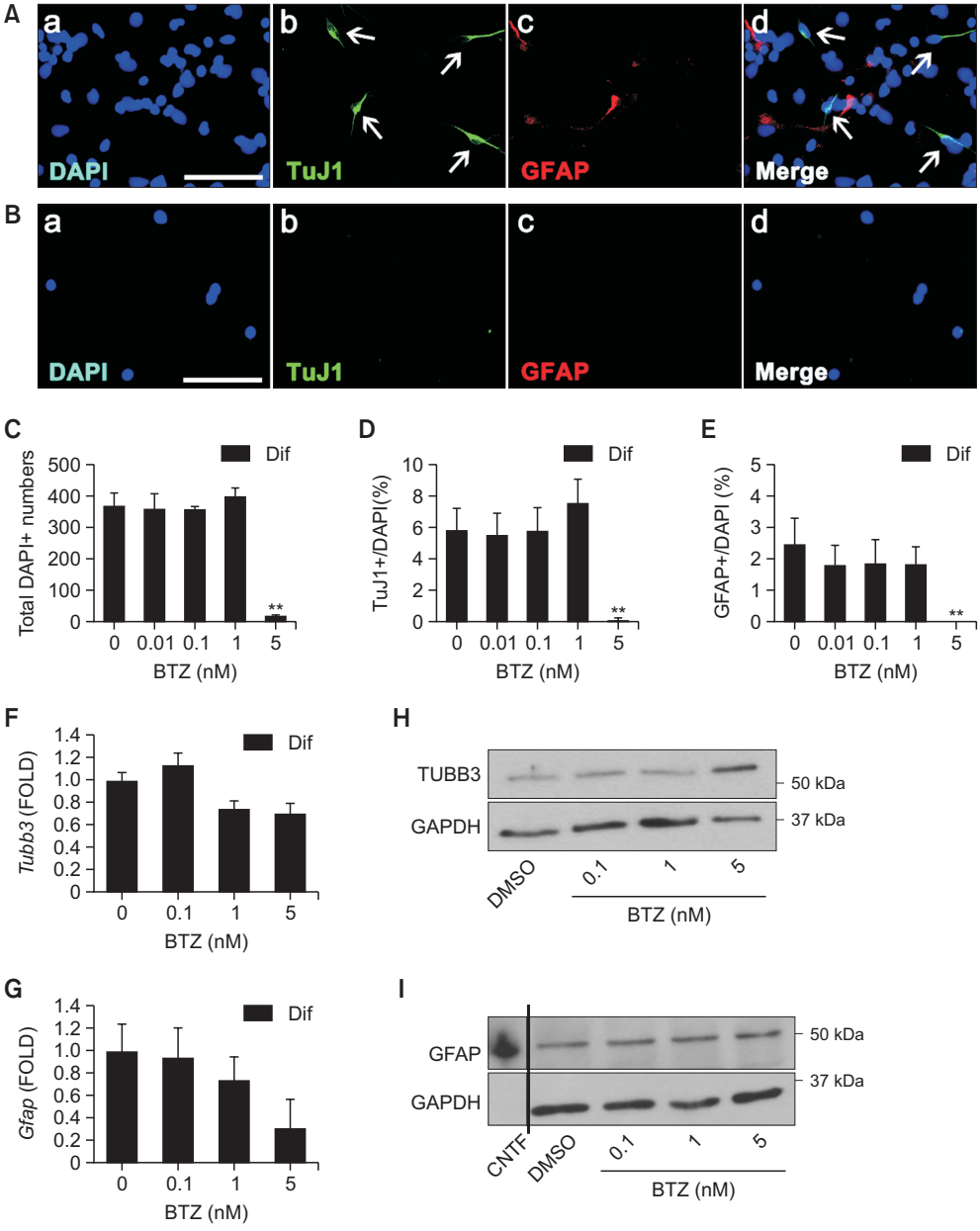

Fig. 2. BTZ increases TUBB3 expression in the absence of growth factors. (A-E) NSCs were treated with 0.1% DMSO or 0.01, 0.1, 1, and 5 nM BTZ in the absence of EGF and FGF2 for 4 days. (A, B) Immunofluorescence images of NSCs treated with (A) 0.1% DMSO or (B) 5 nM BTZ showing (a) nuclei stained with DAPI (blue), (b) neurons stained with TuJ1 (green), (c) astrocytes stained with GFAP (red), and (d) the merged images. Neurons are indicated by arrows (→). Scale bar=50 μm. (C-E) Quantification of (C) nuclei, (D) TuJ1- and (E) GFAP-positive cells. (F, G) RT-PCR was performed to quantify mRNA levels of *Tubb3* and *Gfap*. Total RNA was extracted from NSCs treated with 0.1% DMSO or 0.1, 1, and 5 nM BTZ for 48 h in the absence of EGF and FGF2. *Gapdh* was used as an internal control. (H, I) Representative images of protein bands of (H) TUBB3 and (I) GFAP. After 48 h of treatment in the absence of EGF and FGF2, total cell lysates were collected, and a western blot analysis was conducted with TuJ1 and GFAP antibodies. GAPDH was used as a loading control. CNTF was used as a positive control for GFAP. Data are presented as the mean ± SEM (n=3). ***p*<0.01 (Student's *t*-test). Uncropped images of western blots are shown in Supplementary Fig. 2.

These data suggest that in the presence of EGF and FGF2, neurogenesis appears to be induced by BTZ (5 nM), although 5 nM BTZ is decreasing the cell number. Our results also indicate that TUBB3 degradation is blocked by BTZ (5 nM) in both proliferating NSCs and differentiated cells.

Next, we obtained time-lapse images of NSCs treated with 5 nM BTZ in the presence of mitogens. Time-lapse microscopy showed that a single NSC, rounded up and resulted in two daughter cells between 6 h 40 m and 7 h 00 m (Fig. 3A, 3B). One of the two divided cells was detected to express neuronal marker protein TUBB3, which is determined by TUJ1 immunostaining (Fig. 3C, 3D). Our data suggest that even though

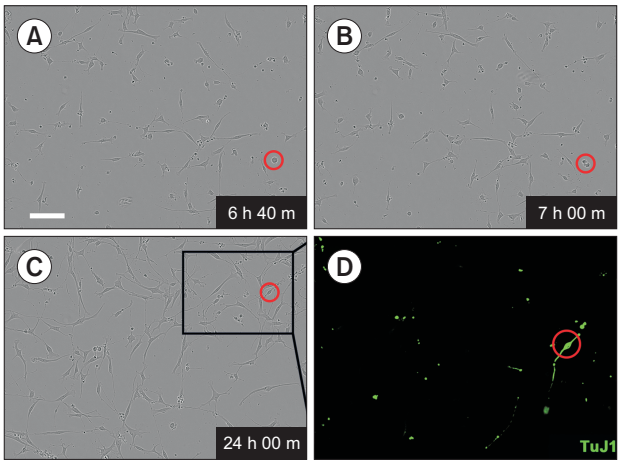

Fig. 3. Time-lapse images of BTZ treated NSCs. BTZ-treated NSCs round up, divide and express neuronal marker protein in the presence of mitogens. (A-C) Time-lapse microscopic photos of BTZ treated NSCs were taken every 20 min. (A, B) A cell marked in a red circle rounded up (A), and divided into two daughter cells (B). One of the daughter cells (C) differentiated into a neuron as determined by immunocytochemistry using TuJ1 (D, Green). Time-stamp indicates the elapsed time from BTZ treatment. Scale bar=100 μm.

BTZ is cytotoxic, it induces neurogenesis from NSCs in the presence of EGF and FGF2.

BTZ induces cell death to NSCs and reduces Bcl-2/Bax ratio

To explore the effect of BTZ on NSC proliferation, we measured the size of the neurospheres in BTZ-treated NSCs in the presence of EGF/FGF2. The diameter of each neurosphere was measured under a microscope every day for 4 days. As shown in Fig. 4A and 4B, the volume of 5 nM BTZ-treated neurospheres was significantly reduced from the 2nd day, compared with that of control. To investigate whether the reduction of neurosphere size is due to inducing of cell death or inhibition of proliferation, we measured the ratio of Bcl-2/Bax mRNA and protein expression by PCR and western blot, respectively (Fig. 4C-4H). BTZ significantly reduced the Bcl-2/Bax transcripts and protein ratio in both proliferating NSCs and differentiating cells (Fig. 4C-4H). Our data indicate that 5 nM BTZ induces cell death in both NSCs and differentiated cells.

BTZ enhances phosphorylation of CREB in NSCs and induces BDNF expression in NSCs and differentiated cells

Next, we explored the mechanisms of increased neurogenesis in NSCs by BTZ. As shown in Fig. 5A and 5B, BTZ (5 nM) dramatically increased poly-ubiquitinated proteins in both NSCs and differentiated cells after 12 h of treatment. These data showed that BTZ inhibited the proteasomes. Next, we measured BDNF expression and CREB activation which are involved in neurogenesis. BTZ (5 nM) increased the protein level of BDNF in NSC proliferation and differentiation condition (Fig. 5C, 5D). Increased CREB phosphorylation was observed in proliferating NSCs but not in differentiated cells (Fig. 5E-5H). Because BTZ is a PI, the up-regulation of BDNF might be due to the inhibition of protein degradation. Thus, we performed RT-PCR experiments to identify whether the increase of BDNF was due to the inhibition of proteasome function or due to transcriptional activation. Interestingly, as shown in Fig. 5I and 5J, 5 nM BTZ significantly up-regulated *Bdnf* mRNA levels only in proliferating NSCs. Although *Bdnf* transcript levels increased in the differentiated cells, it was not statistically significant (p value=0.08). These suggest that the induction of BDNF is not simply due to the inhibition of protein degradation but also by activation of BDNF transcription in the presence of mitogens.

BTZ induces cell death without affecting TUBB3 expression in undifferentiated SH-SY5Y cells

Since BTZ induced cellular death and increased neurogenesis in NSCs, we decided to test whether similar effects can be observed in other types of neural cells. We treated human neuroblastoma SH-SY5Y cells with BTZ, without inducing differentiation to mimic NSCs status, and performed an MTT assay and western blot analysis. The MTT assay revealed that doses of BTZ over 5 nM reduced cell viability of SH-SY5Y cells after 48 h (Fig. 6A, 6B). When the expression levels of TUBB3 and GFAP were determined by western blot analysis, TUBB3 expression remained unchanged in BTZ-treated SH-SY5Y cells, and GFAP was not detected (Fig. 6C, 6D). BTZ decreased the BCL-2/BAX ratio, and reduced CREB phosphorylation (Fig. 6E-6H). However, BTZ treatment increased BDNF protein expression (Fig. 6I, 6J). Interestingly, the mRNA level of *Bdnf* was significantly reduced in BTZ-treated SH-SY5Y cells (Fig. 6K). Our results suggest that BTZ is inducing cell death in NSCs, differentiated cells and undifferentiated SH-SY5Y cells, however, BTZ only enhances neurogenesis in proliferating NSCs. CREB phosphorylation and transcriptional activation of *Bdnf* by BTZ were also only observed in NSCs during proliferation but not in undifferentiated SH-SY5Y cells.

DISCUSSION

BTZ is a PI and is used to treat MM and immune diseases (Scheibe *et al*., 2017; Zhang *et al*., 2017). However, due to PN induction, the use of BTZ has been complicated in MM (Li *et al*., 2020; Selvy *et al*., 2021; Yan *et al*., 2021). Therefore, in this study, we explored whether BTZ induces neurotoxicity and alters NSC fate. We found that 5 nM BTZ induced cell death to both NSCs and differentiated cells determined via immunostaining, cell counting, and the Bcl-2/Bax protein ratio. Interestingly, we have observed the differential effects of 5 nM BTZ on NSCs depending on the presence of growth factors. Although BTZ induces cell death, in the presence of EGF and FGF2, BTZ increased neurogenesis. Since BTZ is a PI, we expected to see an increase in TUBB3 protein levels; however, the transcript level of *Tubb3* was also increased. These suggest that BTZ indeed increases neurogenesis in NSCs, especially in the presence of mitogens. With time-lapse microscopy, we have observed that after BTZ treatment, NSCs rounded up and divided and turned into neurons in the presence of mitogens. We have previously reported that neurogenesis occurs through the final cell division of NSCs (Kim *et al*., 2007).

It should be noted that although the percentage of neurons increased, the neurons were sparse. Because BTZ induces cell death to NSCs, it is possible that the induction of neurogenesis might be a response to replace the lost neurons. Our results that BTZ induces cell death but has a role in the

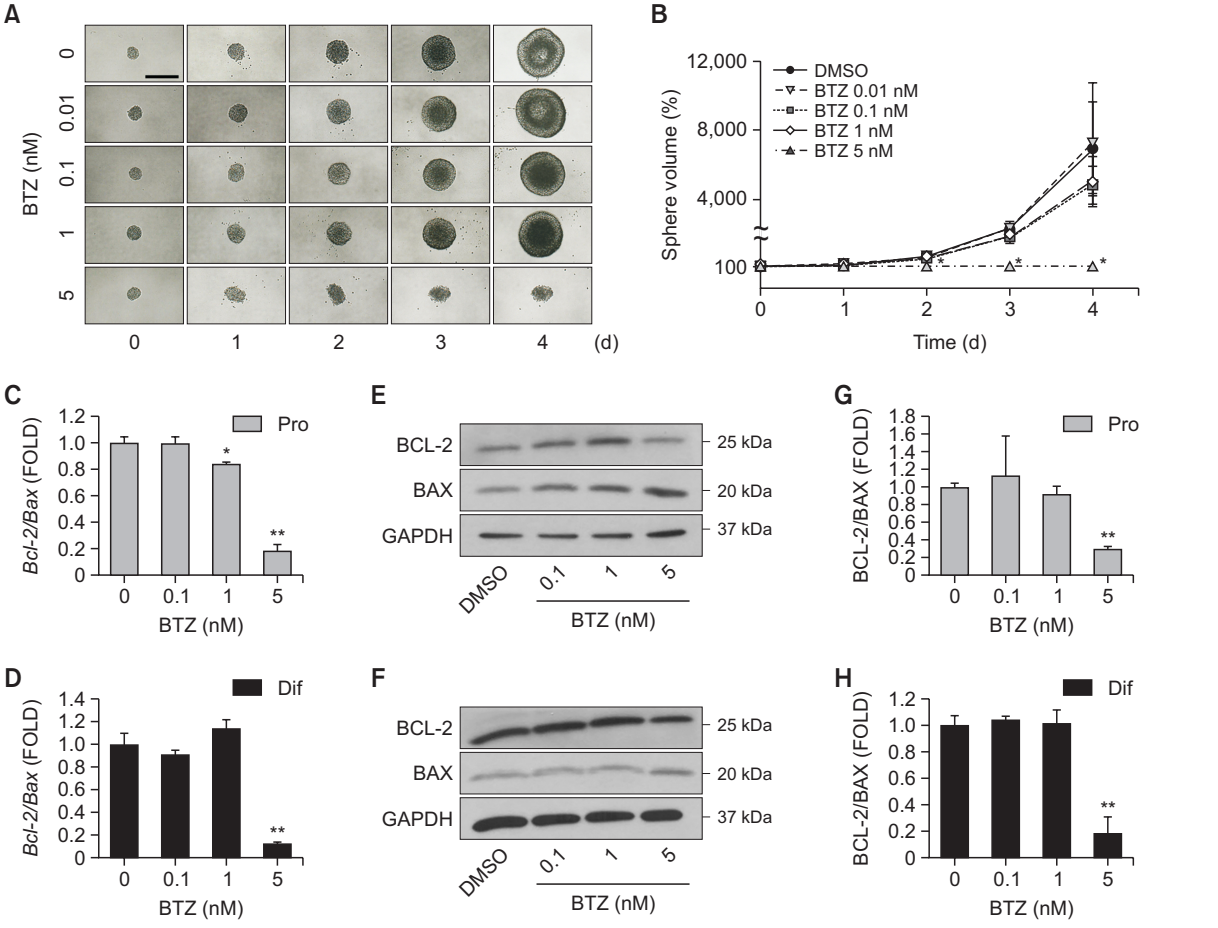

Fig. 4. BTZ obstructs NSC proliferation in the presence of growth factors and reduces Bcl-2/Bax ratio to induce apoptosis. (A) Images of neurospheres treated with 0.1% DMSO or 0.01, 0.1, 1, and 5 nM BTZ for 4 days in the presence of growth factors. Scale bar=250 μm. (B) The volume of neurospheres was estimated by measuring the diameter of individual neurospheres treated with DMSO or BTZ. (C, D) RT-PCR was performed to quantify mRNA level ratio of *Bcl-2* to *Bax*. Total RNA was extracted from NSCs treated with DMSO or BTZ (0.1-5 nM) for (C) 24 h in proliferation media or (D) 48 h in differentiation media. *Gapdh* was used as an internal control. (E, F) Representative images of protein bands of BCL-2 and BAX. Cell lysates were collected from NSCs treated with DMSO or BTZ (0.1-5 nM) for (E) 24 h in proliferation media or (F) 48 h in differentiation media, and a western blot analysis was conducted with BCL-2 and BAX antibodies. (G, H) Densitometer graphs of BCL-2/BAX protein expression. GAPDH was used as a loading control. Data are presented as the mean ± SEM (n=3). **p*<0.05, ***p*<0.01 (Student's *t*-test). Uncropped images of western blots are shown in Supplementary Fig. 3.

induction of neurons are supported by other studies (Romero-Granados *et al*., 2011; Doeppner *et al*., 2016). PI treatments increased neurotoxicity in post-natal mice; however, in an acute stroke animal model, intraperitoneal injection of the PI, BSc2118 enhanced neuronal survival (Romero-Granados *et al*., 2011; Doeppner *et al*., 2016). We also have previously reported that MG132, a different PI, induced cell death but increased the percentage of neurons suggesting that neurons are the least affected cells by PIs (Kim and Kim, 2020). Interestingly, the induction of neurogenesis by BTZ occurred only in proliferating NSCs. In undifferentiated SH-SY5Y cells, BTZ induced cell death without affecting differentiation or increasing the transcription of Tubb3 mRNA. Similar to our results, it has been reported that BTZ increased cytotoxicity in neuroblastoma cells, and BTZ has been suggested as a cancer treatment in combination with other traditional anti-cancer drugs (Brignole *et al*., 2006; Michaelis *et al*., 2006; Du *et al*., 2012).

BTZ is known to regulate bone differentiation and has been reported to increase osteogenesis in mesenchymal stem cells (MSCs) (Giuliani *et al*., 2007; Mukherjee *et al*., 2008; Zhang *et al*., 2020). Similar to our results, although toxic to MSC, low concentrations of BTZ were shown to induce MSC differentiation (Zhang *et al*., 2020). Osteogenic differentiation caused by BTZ appeared to be regulated by $p21^{Cip1}$ and $p27^{Kip1}$ that are transcriptionally activated by BTZ (Zhang *et al*., 2020). These results and our data suggest that BTZ functions not only as a PI but also has a role in signal transduction and activates genes that are important for differentiation. However, it is possible that the induction of differentiation might be due to the regulation of the stability of transcription factors such as Gli3 and Runx2 that mediates osteogenesis (Mukherjee *et al*., 2008). In this study, we showed that, in the absence of EGF and FGF2, 5 nM BTZ treatment was inducing cell death and did not induce neurogenesis. Induction of BDNF and TUBB3 in NSCs suggest that during proliferation, the neurogenesis

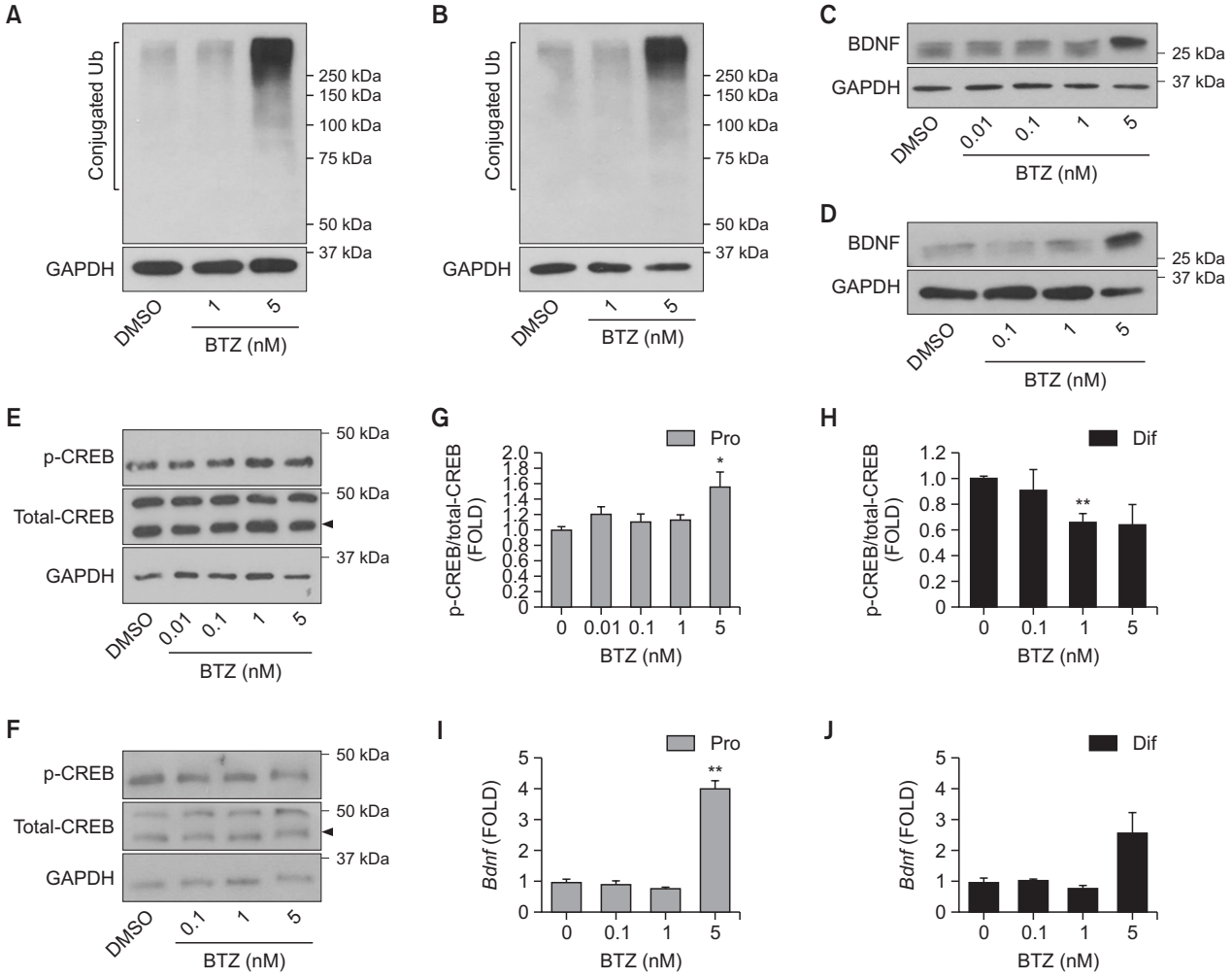

Fig. 5. BTZ increases BDNF expression and phosphorylation of CREB in proliferating NSCs. (A, B) Representative images of the protein bands showing ubiquitin. NSCs were treated with 0.1% DMSO or 1 and 5 nM BTZ for 12 h (A) supplemented with growth factors for proliferation or (B) in the absence of growth factors for differentiation. After 12 h, total cell lysates were collected, and a western blot analysis was conducted with ubiquitin antibodies. Images of protein bands representing (C, D) BDNF and (E, F) p-CREB are shown. (G, H) Densitometer graphs of p-CREB expression. NSCs were treated with (C, E, G) 0.1% DMSO or BTZ (0.01-5 nM) for 24 h in proliferation media and (D, F, H) 0.1% DMSO or BTZ (0.1-5 nM) for 48 h in differentiation media. After treatment, cell lysates were progressed to western blot analysis with BDNF and p-CREB antibodies. GAPDH and total-CREB were used as loading controls. (I, J) RT-PCR was performed to quantify mRNA levels of *Bdnf*. Total RNA was extracted from NSCs treated with 0.1% DMSO or BTZ (0.1-5 nM) for (I) 24 h in proliferation media and (J) 48 h in differentiation media. *Gapdh* was used as an internal control. Data are shown as the mean ± SEM (n=3). **p*<0.05, ***p*<0.01 (Student's *t*-test). Uncropped images of western blots are shown in Supplementary Fig. 4, 5, and 6.

signaling pathway is activated by BTZ. It is plausible that BTZ enhanced the stability of the transcription factors that are involved in neurogenesis and resulted in the induction of neurons in proliferating NSCs.

Interestingly, only TUBB3 but not GFAP protein degradation was affected by BTZ. It has been known that proteolytic signal sequences that are enriched with proline (P), glutamic acid (E), serine (S), and threonine (T; PEST sequences), play an important role in proteasome-mediated degradation of the proteins (Rechsteiner and Rogers, 1996). Proteins that are prone to degrade rapidly, such as Myc, Fos, and p53 contain PEST sequences (Ciechanover *et al*., 1991; Rechsteiner, 1991; Tsurumi *et al*., 1995; Rechsteiner and Rogers, 1996). When we ran the epestfind (https://emboss.bioinformatics.nl/cgi-bin/emboss/epestfind) program, we have found that only TUBB3 has a PEST sequence (PEST score 9.64) at the C terminus (Supplementary Fig. 11). It has been reported that a PEST score greater than zero suggests potential PEST motif (Rechsteiner and Rogers, 1996). In our analysis, the potential PEST motif of TUBB3 was found between the amino acids position 396 and 450. In GFAP protein, no such PEST sequence was found. It has been reported that PEST sequences embedded in proteins such as Notch1, Hax1, and NANOG are responsible for proteasome-mediated degradation (Oberg *et al*., 2001; Ramakrishna *et al*., 2011; Li *et al*., 2012). Therefore, we assume that the C-terminus PEST sequence found in TUBB3 plays an essential role in proteasome-mediated degradation, and because of this, only TUBB3 but not GFAP proteolysis is inhibited by BTZ treatment.

Low concentrations of BTZ in the presence of mitogens

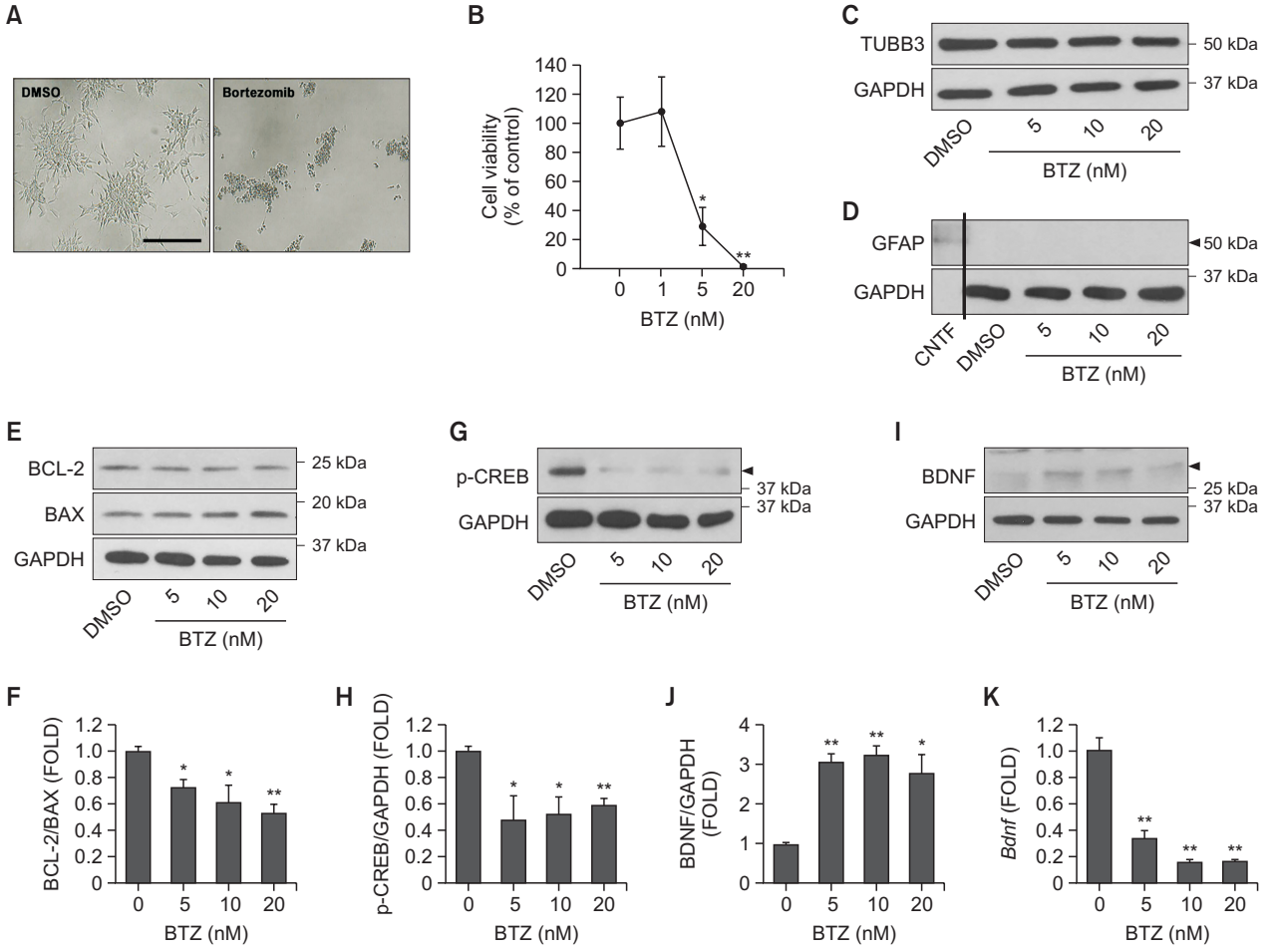

Fig. 6. BTZ induces cell death in undifferentiated SH-SY5Y cells but has no significant effect on TUBB3 level. (A, B) SH-SY5Y cells were treated with 0.1% DMSO or 1, 5, and 20 nM BTZ for 48 h. (A) The representative images present the cell density and morphology of SH-SY5Y cells treated with DMSO and BTZ (20 nM). Scale bar=250 μm. (B) MTT assay was used to measure cell viability. (C-J) SH-SY5Y cells were treated with 0.1% DMSO or 5, 10, and 20 nM BTZ for 36 h. After treatment, total cell lysates were collected, and a western blot analysis was conducted. (C, D) Representative images of protein bands showing (C) TUBB3 and (D) GFAP. Representative images of protein bands with their respective densitometer graph (E, F) BCL-2/BAX ratio, (G, H) p-CREB, and (I, J) BDNF. GAPDH was used as loading controls. CNTF was used as a positive control for GFAP. (K) RT-PCR was performed to quantify *Bdnf* mRNA levels. Total RNA was extracted from SH-SY5Y cells treated with 0.1% DMSO or 5, 10, and 20 nM BTZ for 24 h. *Gapdh* was used as an internal control. Data are shown as the mean ± SEM (n=3). **p*<0.05, ***p*<0.01 (Student's *t*-test). Images of SH-SY5Y cells treated with DMSO and BTZ are shown in Supplementary Fig. 7. Uncropped images of western blots are shown in Supplementary Fig. 8, 9, and 10.

appear to protect neurons in the presence of growth factors, because 1 nM BTZ treatment increased the percentage of neurons shown by ICC but did not increase mRNA and protein expression of TUBB3. It should be noted that clinical dosage of BTZ does not penetrate uninjured blood-brain barrier and only 5-7% of serum levels of BTZ are delivered to the hippocampus and cortex (Huehnchen *et al*., 2020). Despite the fact that BTZ is not easily delivered to the brain, the adverse effects such as cognitive dysfunction in the central nervous system (CNS) have been reported (San Miguel *et al*., 2006). It is possible that aging, inflammation, and diseases in the nervous system would increase the delivery of BTZ to the CNS. In this study, we show that although BTZ is inducing cell death to NSCs and differentiated cells, it not only inhibits proteasome but also induces neurogenesis in the presence of mitogens. Developing reagents that can regulate the proteasome, increase neurogenesis, and decrease cellular toxicity would help to treat MM and neurodegenerative diseases without inducing the adverse effects.

In summary, the PI BTZ enhanced CREB phosphorylation, the mRNA and protein expression levels of BDNF and increased neurogenesis in NSCs (Fig. 7). However, 5 nM BTZ induced cell death to NSCs and differentiated cells. Only TUBB3 contained a potential PEST sequence and the degradation of TUBB3 was inhibited by BTZ treatment in NSCs. Moreover, BTZ reduced cell viability but did not affect TUBB3 expression nor neurogenesis in undifferentiated SH-SY5Y cells. This study suggests that developing PIs with low toxicity and high induction of neurogenesis could be an effective way to treat MM and neurological disorders.

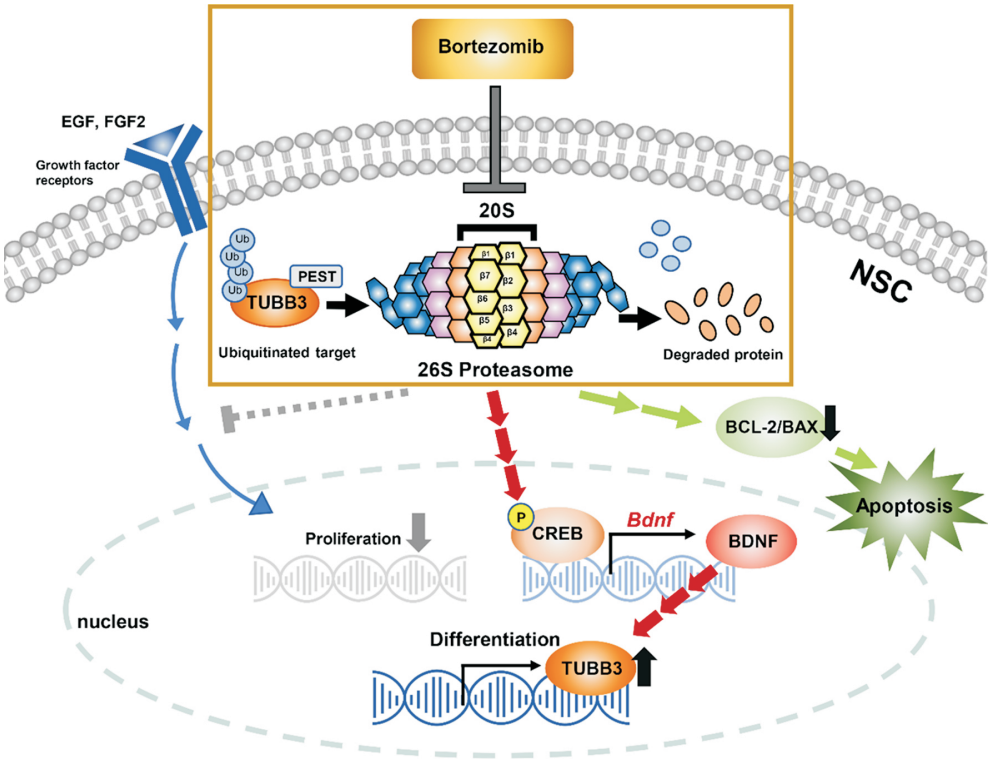

Fig. 7. The PI BTZ induces neurogenesis and apoptosis in NSCs. Proteasome inhibition induced by BTZ increased TUBB3 protein levels in NSCs. In addition, BTZ increased the percentage of neurons and TUBB3 expression by elevating the activation of CREB, *Bdnf* transcripts, and BDNF protein level in proliferating NSCs but not in differentiating NSCs. In contrast, BTZ inhibited the process of NSC proliferation and induced apoptosis by reducing the Bcl-2/Bax ratio.

CONFLICT OF INTEREST

The authors declare that they have no known competing financial interests or personal relationships that could have appeared to influence the work reported in this paper.

ACKNOWLEDGMENTS

This work was done for S.Y. Sohn's Master's degree. This work was supported by Basic Science Research Program through the National Research Foundation of Korea (NRF) funded by the Ministry of Education [grant number 2021R1A6A1A03044296]. This research was supported by the Chung-Ang University Research Scholarship Grants in 2021 (to J.K.).

AUTHOR CONTRIBUTIONS

SYS: Methodology, Validation, Formal analysis, Investigation, Data curation, Visualization, Writing. TTS: Investigation, Data curation, Reviewing, and Editing. JK: Produced revision data. H-JK: Conceptualization, Validation, Writing – original draft, Reviewing and Editing, Visualization, Supervision, Project administration, Funding acquisition.

REFERENCES

Adams, J. (2003) Potential for proteasome inhibition in the treatment of cancer. *Drug Discov. Today* **8**, 307-315.

Bach, S. V. and Hegde, A. N. (2016) The proteasome and epigenetics: zooming in on histone modifications. *Biomol. Concepts* **7**, 215-227.

Brignole, C., Marimpietri, D., Pastorino, F., Nico, B., Di Paolo, D., Cioni, M., Piccardi, F., Cilli, M., Pezzolo, A., Corrias, M. V., Pistoia, V., Ribatti, D., Pagnan, G. and Ponzoni, M. (2006) Effect of bortezomib on human neuroblastoma cell growth, apoptosis, and angiogenesis. *J. Natl. Cancer Inst.* **98**, 1142-1157.

Chen, D. and Dou, Q. P. (2010) The ubiquitin-proteasome system as a prospective molecular target for cancer treatment and prevention. *Curr. Protein Pept. Sci.* **11**, 459-470.

Ciechanover, A. (2005) Intracellular protein degradation: from a vague idea thru the lysosome and the ubiquitin-proteasome system and onto human diseases and drug targeting. *Cell Death Differ.* **12**, 1178-1190.

Ciechanover, A., DiGiuseppe, J. A., Bercovich, B., Orian, A., Richter, J. D., Schwartz, A. L. and Brodeur, G. M. (1991) Degradation of nuclear oncoproteins by the ubiquitin system *in vitro*. *Proc. Natl. Acad. Sci. U. S. A.* **88**, 139-143.

Cohen-Kaplan, V., Livneh, I., Avni, N., Cohen-Rosenzweig, C. and Ciechanover, A. (2016) The ubiquitin-proteasome system and autophagy: Coordinated and independent activities. *Int. J. Biochem. Cell Biol.* **79**, 403-418.

Dick, L. R. and Fleming, P. E. (2010) Building on bortezomib: second-generation proteasome inhibitors as anti-cancer therapy. *Drug Discov. Today* **15**, 243-249.

Doeppner, T. R., Kaltwasser, B., Kuckelkorn, U., Henkelein, P., Bretschneider, E., Kilic, E. and Hermann, D. M. (2016) Systemic proteasome inhibition induces sustained post-stroke neurological

recovery and neuroprotection via mechanisms involving reversal of peripheral immunosuppression and preservation of blood-brain-barrier integrity. *Mol. Neurobiol.* **53**, 6332-6341.

Du, B. Y., Song, W., Bai, L., Shen, Y., Miao, S. Y. and Wang, L. F. (2012) Synergistic effects of combination treatment with bortezomib and doxorubicin in human neuroblastoma cell lines. *Chemotherapy* **58**, 44-51.

Giuliani, N., Morandi, F., Tagliaferri, S., Lazzaretti, M., Bonomini, S., Crugnola, M., Mancini, C., Martella, E., Ferrari, L., Tabilio, A. and Rizzoli, V. (2007) The proteasome inhibitor bortezomib affects osteoblast differentiation *in vitro* and *in vivo* in multiple myeloma patients. *Blood* **110**, 334-338.

Huehnchen, P., Springer, A., Kern, J., Kopp, U., Kohler, S., Alexander, T., Hiepe, F., Meisel, A., Boehmerle, W. and Endres, M. (2020) Bortezomib at therapeutic doses poorly passes the blood-brain barrier and does not impair cognition. *Brain Commun.* **2**, fcaa021.

Kaushik, S. and Cuervo, A. M. (2015) Proteostasis and aging. *Nat. Med.* **21**, 1406-1415.

Kim, H. J., McMillan, E., Han, F. and Svendsen, C. N. (2009) Regionally specified human neural progenitor cells derived from the mesencephalon and forebrain undergo increased neurogenesis following overexpression of ASCL1. *Stem Cells* **27**, 390-398.

Kim, H. J., Sugimori, M., Nakafuku, M. and Svendsen, C. N. (2007) Control of neurogenesis and tyrosine hydroxylase expression in neural progenitor cells through bHLH proteins and Nurr1. *Exp. Neurol.* **203**, 394-405.

Kim, Y. M. and Kim, H. J. (2020) Proteasome inhibitor MG132 is toxic and inhibits the proliferation of rat neural stem cells but increases BDNF expression to protect neurons. *Biomolecules* **10**, 1507.

Kong, S. Y., Kim, W., Lee, H. R. and Kim, H. J. (2018) The histone demethylase KDM5A is required for the repression of astrocytogenesis and regulated by the translational machinery in neural progenitor cells. *FASEB J.* **32**, 1108-1119.

Kong, S. Y., Park, M. H., Lee, M., Kim, J. O., Lee, H. R., Han, B. W., Svendsen, C. N., Sung, S. H. and Kim, H. J. (2015) Kuwanon V inhibits proliferation, promotes cell survival and increases neurogenesis of neural stem cells. *PLoS One* **10**, e0118188.

Lee, H. R., Ann, J., Kim, Y. M., Lee, J. and Kim, H. J. (2021) The KDM5 inhibitor KDM5-C70 induces astrocyte differentiation in rat neural stem cells. *ACS Chem. Neurosci.* **12**, 441-446.

Lee, H. R., Farhanullah, Lee, J., Jajoo, R., Kong, S. Y., Shin, J. Y., Kim, J. O., Lee, J., Lee, J. and Kim, H. J. (2016) Discovery of a small molecule that enhances astrocytogenesis by activation of STAT3, SMAD1/5/8, and ERK1/2 via induction of cytokines in neural stem cells. *ACS Chem. Neurosci.* **7**, 90-99.

Lee, H. R., Lee, J. and Kim, H. J. (2019) Differential effects of MEK inhibitors on rat neural stem cell differentiation: repressive roles of MEK2 in neurogenesis and induction of astrocytogenesis by PD98059. *Pharmacol. Res.* **149**, 104466.

Li, B., Hu, Q., Xu, R., Ren, H., Fei, E., Chen, D. and Wang, G. (2012) Hax-1 is rapidly degraded by the proteasome dependent on its PEST sequence. *BMC Cell Biol.* **13**, 20.

Li, T., Timmins, H. C., King, T., Kiernan, M. C., Goldstein, D. and Park, S. B. (2020) Characteristics and risk factors of bortezomib induced peripheral neuropathy: a systematic review of phase III trials. *Hematol. Oncol.* **38**, 229-243.

Martinez-Vicente, M., Sovak, G. and Cuervo, A. M. (2005) Protein degradation and aging. *Exp. Gerontol.* **40**, 622-633.

Michaelis, M., Fichtner, I., Behrens, D., Haider, W., Rothweiler, F., Mack, A., Cinatl, J., Doerr, H. W. and Cinatl, J., Jr. (2006) Anti-cancer effects of bortezomib against chemoresistant neuroblastoma cell lines *in vitro* and *in vivo*. *Int. J. Oncol.* **28**, 439-446.

Mukherjee, S., Raje, N., Schoonmaker, J. A., Liu, J. C., Hideshima, T., Wein, M. N., Jones, D. C., Vallet, S., Bouxsein, M. L., Pozzi, S., Chhetri, S., Seo, Y. D., Aronson, J. P., Patel, C., Fulciniti, M., Purton, L. E., Glimcher, L. H., Lian, J. B., Stein, G., Anderson, K. C. and Scadden, D. T. (2008) Pharmacologic targeting of a stem/progenitor population *in vivo* is associated with enhanced bone regeneration in mice. *J. Clin. Invest.* **118**, 491-504.

Nam, T., Han, J. H., Devkota, S. and Lee, H. W. (2017) Emerging paradigm of crosstalk between autophagy and the ubiquitin-proteasome system. *Mol. Cells* **40**, 897-905.

Oberg, C., Li, J., Pauley, A., Wolf, E., Gurney, M. and Lendahl, U. (2001) The Notch intracellular domain is ubiquitinated and negatively regulated by the mammalian Sel-10 homolog. *J. Biol. Chem.* **276**, 35847-35853.

Paul, S. (2008) Dysfunction of the ubiquitin-proteasome system in multiple disease conditions: therapeutic approaches. *Bioessays* **30**, 1172-1184.

Pero, M. E., Meregalli, C., Qu, X., Shin, G. J., Kumar, A., Shorey, M., Rolls, M. M., Tanji, K., Brannagan, T. H., Alberti, P., Fumagalli, G., Monza, L., Grueber, W. B., Cavaletti, G. and Bartolini, F. (2021) Pathogenic role of delta 2 tubulin in bortezomib-induced peripheral neuropathy. *Proc. Natl. Acad. Sci. U. S. A.* **118**, e2012685118.

Pohl, C. and Dikic, I. (2019) Cellular quality control by the ubiquitin-proteasome system and autophagy. *Science* **366**, 818-822.

Poruchynsky, M. S., Sackett, D. L., Robey, R. W., Ward, Y., Annunziata, C. and Fojo, T. (2008) Proteasome inhibitors increase tubulin polymerization and stabilization in tissue culture cells: a possible mechanism contributing to peripheral neuropathy and cellular toxicity following proteasome inhibition. *Cell Cycle* **7**, 940-949.

Ramakrishna, S., Suresh, B., Lim, K. H., Cha, B. H., Lee, S. H., Kim, K. S. and Baek, K. H. (2011) PEST motif sequence regulating human NANOG for proteasomal degradation. *Stem Cells Dev.* **20**, 1511-1519.

Rechsteiner, M. (1991) Natural substrates of the ubiquitin proteolytic pathway. *Cell* **66**, 615-618.

Rechsteiner, M. and Rogers, S. W. (1996) PEST sequences and regulation by proteolysis. *Trends Biochem. Sci.* **21**, 267-271.

Richardson, P. G., Xie, W., Mitsiades, C., Chanan-Khan, A. A., Lonial, S., Hassoun, H., Avigan, D. E., Oaklander, A. L., Kuter, D. J., Wen, P. Y., Kesari, S., Briemberg, H. R., Schlossman, R. L., Munshi, N. C., Heffner, L. T., Doss, D., Esseltine, D. L., Weller, E., Anderson, K. C. and Amato, A. A. (2009) Single-agent bortezomib in previously untreated multiple myeloma: efficacy, characterization of peripheral neuropathy, and molecular correlations with response and neuropathy. *J. Clin. Oncol.* **27**, 3518-3525.

Robak, P. and Robak, T. (2019) Bortezomib for the treatment of hematologic malignancies: 15 years later. *Drugs R. D.* **19**, 73-92.

Romero-Granados, R., Fontan-Lozano, A., Aguilar-Montilla, F. J. and Carrion, A. M. (2011) Postnatal proteasome inhibition induces neurodegeneration and cognitive deficiencies in adult mice: a new model of neurodevelopment syndrome. *PLoS One* **6**, e28927.

San Miguel, J., Blade, J., Boccadoro, M., Cavenagh, J., Glasmacher, A., Jagannath, S., Lonial, S., Orlowski, R. Z., Sonneveld, P. and Ludwig, H. (2006) A practical update on the use of bortezomib in the management of multiple myeloma. *Oncologist* **11**, 51-61.

Scheibe, F., Pruss, H., Mengel, A. M., Kohler, S., Numann, A., Kohnlein, M., Ruprecht, K., Alexander, T., Hiepe, F. and Meisel, A. (2017) Bortezomib for treatment of therapy-refractory anti-NMDA receptor encephalitis. *Neurology* **88**, 366-370.

Selvy, M., Kerckhove, N., Pereira, B., Barreau, F., Nguyen, D., Busserolles, J., Giraudet, F., Cabrespine, A., Chaleteix, C., Soubrier, M., Bay, J. O., Lemal, R. and Balayssac, D. (2021) Prevalence of chemotherapy-induced peripheral neuropathy in multiple myeloma patients and its impact on quality of life: a single center cross-sectional study. *Front. Pharmacol.* **12**, 637593.

Thibaudeau, T. A. and Smith, D. M. (2019) A practical review of proteasome pharmacology. *Pharmacol. Rev.* **71**, 170-197.

Tsurumi, C., Ishida, N., Tamura, T., Kakizuka, A., Nishida, E., Okumura, E., Kishimoto, T., Inagaki, M., Okazaki, K., Sagata, N., Ichihara, A. and Tanaka, K. (1995) Degradation of c-Fos by the 26S proteasome is accelerated by c-Jun and multiple protein kinases. *Mol. Cell. Biol.* **15**, 5682-5687.

Velasco, R., Alberti, P., Bruna, J., Psimaras, D. and Argyriou, A. A. (2019) Bortezomib and other proteosome inhibitors-induced peripheral neurotoxicity: from pathogenesis to treatment. *J. Peripher. Nerv. Syst.* **24 Suppl 2**, S52-S62.

Velasco, R., Petit, J., Clapes, V., Verdu, E., Navarro, X. and Bruna, J. (2010) Neurological monitoring reduces the incidence of bortezomib-induced peripheral neuropathy in multiple myeloma patients. *J. Peripher. Nerv. Syst.* **15**, 17-25.

Vilchez, D., Saez, I. and Dillin, A. (2014) The role of protein clearance mechanisms in organismal ageing and age-related diseases. *Nat.*

Commun. **5**, 5659.
Yan, W., Wu, Z., Zhang, Y., Hong, D., Dong, X., Liu, L., Rao, Y., Huang, L., Zhang, X. and Wu, J. (2021) The molecular and cellular insight into the toxicology of bortezomib-induced peripheral neuropathy. *Biomed. Pharmacother.* **142**, 112068.
Ye, Y. (2018) Regulation of protein homeostasis by unconventional protein secretion in mammalian cells. *Semin. Cell Dev. Biol.* **83**, 29-35.
Zhang, C., Tian, D. C., Yang, C. S., Han, B., Wang, J., Yang, L. and Shi, F. D. (2017) Safety and efficacy of bortezomib in patients with highly relapsing neuromyelitis optica spectrum disorder. *JAMA Neurol.* **74**, 1010-1012.
Zhang, D., Fan, R., Lei, L., Lei, L., Wang, Y., Lv, N., Chen, P., Williamson, R. A., Wang, B. and Hu, J. (2020) Cell cycle exit during bortezomib-induced osteogenic differentiation of mesenchymal stem cells was mediated by Xbp1s-upregulated p21(Cip1) and p27(Kip1). *J. Cell. Mol. Med.* **24**, 9428-9438.